JPET Fast Forward. Published on October 18, 2006 as DOI: 10.1124/jpet.106.112581

JPET #112581

Title Page

Ca^{2+}-calmodulin and Jak2 are Required for Activation of Sodium-proton Exchange by the G_i-coupled 5-hydroxytryptamine$_{1A}$ Receptor

Justin N. Turner, Maria N. Garnovskaya, Sonya D. Coaxum, Tamara M. Vlasova, Margarita Yakutovich, David M. Lefler, and John R. Raymond

The Medical and Research Services of the Ralph H. Johnson Veterans Affairs Medical Center, and Department of Medicine (Nephrology Division) of the Medical University of South Carolina, Charleston, S.C., 29425

JPET Fast Forward. Published on October 18, 2006 as DOI: 10.1124/jpet.106.112581
This article has not been copyedited and formatted. The final version may differ from this version.

Running Title Page

Running title: Calmodulin, Jak2, and NHE-1

Address correspondence to Dr. John Raymond, 179 Ashley Avenue, Office of the Provost, Charleston, SC, 29425. Ph; 1-(843)-792-3031, Fax 1-(843)-792-5110, raymondj@musc.edu.

# of Text Pages: 19

# of Tables: 0

# of Figures: 5

# of References: 64

# of Words in Abstract: 226

# of Words in Introduction: 722

# of Words in Discussion: 1,195

Abbreviations used: AG490, N-benzyl-3,4-dihydroxy-benzylidenecyanoacetamide; AG1478, 4-(3-chloroanillino)-6,7-dimethoxyquinazoline; BAPTA, [1,2-bis(2-aminophenoxy)ethane-*N*,*N*,*N'*,*N'*-tetraacetic acid acetoxymethyl ester; BRET, bioluminescence resonance energy transfer; CaM, calcium/calmodulin; CHO, Chinese hamster ovary; daidzein, 7-hydroxy-3- (4-hydroxyphenyl)-4H -1-benzopyran-4-one; ECAR, extracellular acidification rate; eYFP, enhanced yellow fluorescent protein; genistein, 5,7-dihydroxy-3-(4-hydroxyphenyl)-4H-1-benzopyran-4-one; GFP, green fluorescent protein; G protein, guanine nucleotide binding regulatory protein; 5-HT, 5-hydroxytryptamine; 5-HT_{1A} receptor, $5\text{-hydroxytryptamine}_{1A}$ receptor; 8-OH-DPAT, 8-hydroxy-2-(di-*n*-propylamino)-tetralin; RLuc, *Renilla reniformis* luciferase; NHE-1, type I sodium-proton exchanger; PTX, *Pertussis* toxin; UH-301, 5-fluoro-8 hydroxy-2-(dipropylamino)-tetralin; W-7, N-(6-aminohexyl)5-chloro-1-naphthalene sulfonamide.

Section Assignment: Cellular and Molecular

JPET Fast Forward. Published on October 18, 2006 as DOI: 10.1124/jpet.106.112581
This article has not been copyedited and formatted. The final version may differ from this version.

Abstract

The type I sodium-proton exchanger (NHE-1) is expressed ubiquitously and regulates key cellular functions including mitogenesis, cell volume, and intracellular pH. Despite its importance, the signaling pathways that regulate NHE-1 remain incompletely defined. In this work, we present evidence that stimulation of the 5-hydroxytryptamine$_{1A}$ (5-HT$_{1A}$) receptor results in the formation of a signaling complex that includes activated Jak2, Ca^{2+}/calmodulin (CaM), and NHE-1, and which involves tyrosine phosphorylation of CaM. The signaling pathway also involves rapid agonist-induced association of CaM and NHE-1 as assessed by co-immunoprecipitation studies, and by bioluminescence resonance energy transfer studies in living cells. We propose that NHE-1 is activated through this pathway: 5-HT$_{1A}$ receptor → $G_{i2}\alpha$ and/or $G_{i3}\alpha$ → Jak2 activation → tyrosine phosphorylation of CaM → increased binding of CaM to NHE-1 → induction of a conformational change in NHE-1 that unmasks an obscured proton-sensing and/or proton transporting region of NHE-1 → activation of NHE-1. The $G_{i/o}$-coupled 5-HT$_{1A}$ receptor now joins a handful of G_q-coupled receptors and hypertonic shock as upstream activators of this emerging pathway. In the course of this work, we have presented clear evidence that CaM can be activated through tyrosine phosphorylation in the absence of a significant role for elevated intracellular Ca^{2+}. We have also demonstrated for the first time that the association of CaM with NHE-1 in living cells is a dynamic process.

Introduction

The type-1 sodium-proton exchanger, (NHE-1, also known as product of SLC9A1, solute carrier family 9A, type 1) is ubiquitous, being expressed on the plasma membrane of virtually every mammalian cell. It mediates the 1:1 exchange of extracellular Na^+ for intracellular H^+, thereby maintaining intracellular pH (Pouyssegur et al., 1984; Grinstein et al., 1989). NHE-1 also plays cell-specific roles in the development and maintenance of a transformed cellular phenotype, differentiation of some cell types, structural anchoring and cytoskeletal organization, bone resorption, cell cycle control, apoptosis, and a host of other cellular functions (Putney et al., 2002; Fliegel, 2005). NHE-1 has also been implicated in clinically relevant conditions such as hypertension (Garciandia et al., 1995), left ventricular hypertrophy (Karmazyn et al., 2003), and ischemia-reperfusion injury (Wang et al., 2003). Despite its ubiquitous expression in mammalian cells and its potential clinical relevance, much remains to be learned regarding the molecular mechanisms through which this important protein is regulated.

The structure of NHE-1 suggests that its regulation can occur through at least four mechanisms: (1) interaction of regulatory factor(s) (proteins or lipids) with the cytoplasmic carboxyl terminal region of NHE-1; (2) phosphorylation of serines, threonines and/or tyrosines located in the cytoplasmic domains of NHE-1; (3) phosphorylation of regulatory factors; and/or (4) binding of Ca^{2+}/calmodulin (CaM) to NHE-1 (Counillon and Pouyssegur, 2000). Rapid activation of NHE-1 by mitogens is typically associated with increases in its phosphorylation (Sardet et al., 1991). A variety of protein kinases has been suggested as candidates to regulate NHE-1, including protein kinase C (Sauvage et al., 2000), Ca^{2+}/calmodulin-dependent kinase (Fliegel et al., 1992), myosin light chain kinase (Shrode et al., 1995), p160 Rho-associated kinase (Tominaga et al., 1998), phosphatidylinositol 3'-kinase (Sauvage et al., 2000), the Nck-interacting kinase, NIK (Yan et al., 2001), and members of the mitogen-activated protein kinase (MAPK) family (Takahashi et al., 1999). In VSMC, the 90-kD S6 kinase ($p90^{rsk}$) can directly phosphorylate NHE-1 on Ser-703, and mediate an increase in Na^+-H^+ exchange *in vivo* (Takahashi et al., 1999). However, only half of the response to growth factors is eliminated after

JPET Fast Forward. Published on October 18, 2006 as DOI: 10.1124/jpet.106.112581
This article has not been copyedited and formatted. The final version may differ from this version.

deletion of amino acids 636-815 of NHE-1 (the region with most of the potential phosphorylation sites), indicating that direct phosphorylation of NHE-1 is not essential for its regulation (Wakabayashi et al., 1994b).

Because direct phosphorylation of NHE-1 accounts for only a part of its regulation, we have become interested in alternative pathways of activation, with particular reference to the role of calcium/calmodulin (CaM**).** CaM is a ubiquitous intracellular Ca^{2+} receptor and Ca^{2+}-binding protein. It is a member of the superfamily of EF-hand proteins. CaM has four EF-hand motifs, each of which is composed of two α-helices connected by a 12-amino acid loop. When intracellular Ca^{2+} levels rise to the low micromolar range, all four EF-hands bind Ca^{2+}, inducing a conformational change that results in binding to various target proteins (Crivici and Ikura, 1995). CaM is classically activated by increases in intracellular Ca^{2+}, resulting in conformational changes in CaM and activation of target proteins. However, other mechanisms of regulating CaM are possible, albeit poorly understood. Primary among the alternate mechanisms of activating CaM is phosphorylation of CaM on serine-threonine or tyrosine residues. In that regard, we recently described a novel pathway for the activation of NHE-1 by Jak2 and calmodulin (CaM), through which Jak2-induced phosphorylation of CaM is required for activation of NHE-1 by G_q-coupled receptors and by hypertonic medium (Mukhin et al., 2001; Garnovskaya et al., 2003a; Garnovskaya et al., 2003b). Those findings suggest that G_q-coupled receptors and hypertonic medium stimulate NHE-1 through this pathway: stimulus → Jak2 activation → tyrosine phosphorylation of CaM → binding of CaM to NHE-1 → activation of NHE-1. In the current manuscript, we explore the possibility that a prototypical G_i-coupled receptor, the serotonin 5-HT_{1A} receptor, also utilizes this emerging pathway to activate NHE-1.

.

Methods

Materials

Calmidazolium, fluphenazine, chlorpromazine, W-7, ophiobolin A, BAPTA-AM [1,2-bis(2-aminophenoxy)ethane-*N*,*N*,*N'*,*N'*-tetraacetic acid acetoxymethyl ester], *Pertussis* toxin, and various salts were from Sigma (St Louis, MO). AG490 was from Calbiochem (San Diego, CA). 8-OH-DPAT was from RBI (Natick, MA). Anti-CaM monoclonal antibody, anti-Jak2 agarose conjugated antibody and anti-phosphotyrosine polyclonal antibody were from Upstate Biotechnology (Lake Placid, NY). Total Stat3 and anti-phosphospecific Stat3 (pY705) rabbit antibodies were from Biosource International (Camarillo, CA) or QCB (Hopkinton, MA). Anti-NHE-1 antibody was from Chemicon International (Temecula, CA). All cell culture media and supplements were from Life Sciences (Grand Island, NY). Polycarbonate cell culture inserts for microphysiometry were from Corning Costar (Cambridge, MA). The murine anti-GFP antibody was purchased from Clontech (Mountain View, CA). Goat polycloncal anti-luciferase antibody was obtained from Promega (Madison, WI). Anti-5-HT_{1A} receptor rabbit serum was raised using a peptide sequence from the predicted third intracellular loop of the receptor (G^{242}ASPAPQPKKKSVNGESGSRNWRLGVE), and thoroughly validated and characterized as described (Raymond et al., 1989; Raymond et al., 1993).

Cell Culture

CHO-K1 cells expressing the ≈ 50 fmol of 5-HT_{1A} receptors/mg of protein (CHO-5-HT_{1A}R cells) were maintained in F12/HAMS medium, supplemented with 10% fetal calf serum, streptomycin (100 µg/ml), penicillin (100 units/ml), and gentamycin (400 µg/ml) at 37°C in a 5% CO_2-enriched, humidified atmosphere. 24 to 48 h prior to each experiment, cells were switched to serum-free medium containing 0.5% bovine serum albumin (Sigma).

Microphysiometry

The microphysiometer uses a light addressable silicon sensor to detect extracellular protons (McConnell et al., 1992). Each of eight channels has two inlet ports for buffers, one of which usually contains a vehicle-control, and the other of which carries the test substance. The cells are perfused with buffer, and valve switches and stop-start cycles are totally controlled by a programmable computer. Acidification rate data are transformed by a personal computer running Cytosoft™ version 2.0, and are presented as the extracellular acidification rate in µVolts/sec, which roughly correspond to millipH units/min (Nernst equation). In order to facilitate comparison of data between two channels, values are expressed as a percentage of a baseline determined by computerized analysis of the five data points prior to exposure of the cell monolayers to a test substance.

All experiments were performed as previously described (Garnovskaya et al., 1997; Garnovskaya et al., 2003a; Garnovskaya et al., 2003b). Cells were plated onto polycarbonate membranes (3 micron pore size, 12 µm size) at a density of 300,000 cells per insert the night prior to experimentation. After cells were attached to the membranes, they were growth-arrested in serum-free culture medium for 20 h before the experiment. The day of the study, cells were washed with serum-free, bicarbonate-free Ham's F-12 medium, placed into the microphysiometer chambers, and perfused at 37°C with the same medium or balanced salt solutions. For studies using inhibitors, cells were perfused for 15 minutes with tyrosine kinase inhibitors or CaM inhibitors prior to treatment with 8-OH-DPAT. For most studies, the pump cycle was set to perfuse cells for 60 seconds, followed by a 30 second "pump-off" phase, during which proton efflux was measured from the sixth through the 28th seconds. Cells were exposed to the test agent for three or four cycles (270-360 sec). Valve switches (to add or remove test agents) were performed at the middle of the pump cycle. Data points were then acquired every 90 seconds. The peak effect during stimulation was expressed as the percentage increase from baseline.

Immunoprecipitation

Experiments were performed as previously described (Mukhin et al., 2001; Garnovskaya et al., 2003b). Quiescent cell monolayers were treated with 100 nM 8-OH-DPAT or vehicle for 10 min. In some cases, cells were pre-incubated with 40 μM AG490 for 15 minutes prior to experimentation. After treatment with 8-OH-DPAT or vehicle for 10 minutes, cells were lysed in 1 ml/100 mm dish of RIPA buffer (150 mM NaCl, 50 mM Tris-HCl, pH 7.4, 1 mM EDTA, 1% NP-40, 1 mM NaF, 1 mM Na_3VO_4, 1 mM phenylmethylsulfonyl fluoride, aprotinin, leupeptin and pepstatin at 1 μg/ml of each). Cell lysates were pre-cleared by incubating with a protein A-agarose bead slurry for 30 min at 4°C. Pre-cleared lysates (1 μg/μl total cell protein) were incubated with anti-Jak2/protein A-agarose or with other antibodies overnight (1:20 dilutions) at 4° C. Immunoprecipitates were captured by addition of protein A-agarose. The agarose beads were collected by centrifugation, washed 3 times with RIPA buffer, resuspended in 2× Laemmli sample buffer, boiled for 5 min, and subjected to SDS-PAGE and subsequent immunoblot analysis.

Immunoblotting

The immunoblot protocol used for these studies was identical to that previously described by us (Garnovskaya et al., 2003a), except that the dilutions of the various antibodies followed the manufacturer's recommendations, and that the blots were developed using Vistra ECF reagent (Amersham, Arlington Heights, IL). Dilutions used were: murine anti-GFP (1:1,000), goat anti-luciferase (1:1,000), rabbit anti-Jak2 (1 μg/ml), rabbit anti-phospho-Stat3-pY705 (1:1,000), mouse anti-CaM (1 μg/ml), rabbit anti-NHE-1 (2.5 μg/ml), and rabbit anti-Stat3 (1 μg/ml). In some cases, cells were pre-incubated with inhibitors for 15 minutes prior to experimentation. Cells were incubated with 100 nM 8-OH-DPAT or vehicle for 10 miutes.

Jak2 Phosphorylation Assay

Phosphorylation of Jak2 in response to 8-OH-DPAT was assessed using a Jak2 dual phosphospecific antibody (QCB, Hopkinton, MA). Quiescent cells were treated with 100 nM 8-OH-DPAT for 10 min, and lysed in RIPA buffer. The lysates were subjected to SDS-PAGE under reducing conditions with 4-20% pre-cast gels (Invitrogen, Carlsbad, CA). After semidry transfer to polyvinylidine difluoride membranes, membranes were blocked with a Blotto buffer and incubated with the phospho-Jak2 antibody (0.5 µg/ml). After incubation with alkaline phosphatase-linked secondary antibodies immunoreactive bands were visualized by a chemiluminescent method (CDP Star™, New England BioLabs, Beverly, MA) using pre-flashed Kodak X-AR film, and quantified using a GS-670 densitometer and Molecular Analyst software (BioRad, Hercules, CA).

Immunofluorescence and Confocal Microscopy

Prior to experiments, CHO-5-HT_{1A}R cells were plated in six well plates on collagen I-coated coverslips at 1 x 10^5 cells per well, cultured for 24 h, and then transferred to serum-free F12/HAMS medium supplemented with 0.5% BSA for 24-48 h. Cells were washed twice with ice-cold PBS, and fixed in PBS/4% paraformaldehyde for 30 min. Cells were then permeabilized with PBS/0.2% Triton X-100 for 5 min and incubated with PBS/2% BSA for 30 min to reduce non-specific background staining. To visualize CaM, cells were first incubated with a mouse monoclonal anti-CaM antibody (1:10 dilution) overnight at 4°C. The coverslips were washed 4x for 5 min each with PBS/2% BSA followed by incubation with a TRITC-labeled goat anti-mouse antibody (1:50 dilution) for 30 min at room temperature. Cells were then washed 4x for 5 min each with PBS/2% BSA, then twice for 5 min each with PBS. Coverslips then were mounted on glass slides with Vectashield mounting medium.

JPET Fast Forward. Published on October 18, 2006 as DOI: 10.1124/jpet.106.112581
This article has not been copyedited and formatted. The final version may differ from this version.

Generation of constructs for bioluminescence resonance energy transfer

We generated cDNA constructs in which CaM is tagged in tandem to luciferase by in-frame ligation into the mammalian expression vector, pRL-CMV-*R*luc (Promega). Fusions to the amino terminus of luciferase were termed "RLuc-N1", and to the carboxyl terminus of luciferase were termed "RLuc-C1". Fusions of enhanced yellow fluorescent protein (eYFP) were created by tagging in tandem to the carboxyl terminus of NHE-1, or *vice versa*. This was accomplished by in-frame ligation to the yellow variant GFP-topaz vectors, pGFP-N1-topaz (fusion to the amino terminus of eYFP, "eYFP-N1") or pGFP-C1-topaz (fusion to the carboxyl terminus of eYFP, "eYP-C1") (Biosignal Packard, Montreal, Canada), with or without flexible linker. CHO cells were co-transfected with constructs, and the emissions of light from eYFP and luciferase were measured before and after stimulation with agonist as described previously (Turner et al., 2004; Turner and Raymond, 2005).

Bioluminescence Resonance Energy Transfer

To determine whether CaM and NHE-1 come into close proximity in intact cells, we used bioluminescence resonance energy transfer (BRET), a technique that detects close proximity of proteins using energy transfer between luminescent and fluorescent tags. A bioluminescent donor source (*Renilla reniformis* luciferase, RLuc) can transfer energy to an acceptor flourophore (yellow variant of *Aequorea* green fluorescent protein, YFP) within a radius of approximately 50 Å, and this transfer is virtually undetectable at distances greater than 100 Å (Xu et al., 1999). CHO-5-HT_{1A}R cells were transiently transfected as previously described (Garnovskaya et al., 1997) and cultured in F12/HAMS media for 48 h to allow for protein expression. Cells were detached with PBS/1mM EDTA and distributed into a 96 well plate at 1 x 10^5 cells/well. Fluorescence measurements were acquired using a Victor^2 multilabel plate reader (Perkin Elmer, Shelton, CT). In some cases, cells were incubated with 1 µM 8-OH-DPAT for 5 min. Coelenterazine was then added to a final concentration of 5 µM and sequential

measurements were made with filters at 460 ± 25 nm and 525 ± 25 nm. The BRET ratio was calculated as the ratio of light emitted at 525 nm (eYFP) over the light emitted at 460 nm (luciferase).

Results

8-OH-DPAT activates ERK in CHO fibroblasts expressing the 5-HT$_{1A}$ receptor through CaM and tyrosine kinase(s)

We have previously demonstrated that the 5-HT$_{1A}$ receptor rapidly stimulates NHE-1 in CHO cells (Garnovskaya et al., 1997; Garnovskaya et al., 1998). In Figure 1, we used microphysiometry to demonstrate that activation of NHE-1 is sensitive to inhibitors of Jak2 and CaM. Figure 1A shows representative tracings demonstrating that a CaM inhibitor (1 μM ophiobolin A) reduces the activation of NHE-1 induced by the 5-HT$_{1A}$ receptor agonist, 8-OH-DPAT (100 nM). Figure 1B shows the results of microphysiometry experiments in which a panel of CaM inhibitors was tested for effects on activation of NHE-1 by 100 nM 8-OH-DPAT. Because results obtained with pharmacological inhibitors should be interpreted with caution due to potential non-specific or non-selective effects, we used a panel of diverse CaM inhibitors to probe the involvement of CaM in the activation of NHE-1 by 8-OH-DPAT. Five structurally distinct CaM inhibitors (5 μM calmidazolium; 1 μM ophiobolin A; 50 μM W-7; 10 μM fluphenazine; and 10 μM chlorpromazine) each markedly suppressed the peak activation of NHE-1 by 70-90%. These results suggest that CaM is involved in 5-HT$_{1A}$ receptor-mediated activation of NHE-1. Because one key mechanism through which CaM is activated involves elevation of intracellular Ca^{2+} levels (Crivici and Ikura, 1995), we tested the effect of 50 μM BAPTA-AM, a cell-permeable calcium chelator on 8-OH-DPAT (100 nM)-induced activation of NHE-1. Figure 1B shows that BAPTA-AM had no effect on the activation of NHE-1, suggesting that an alternative pathway is responsible for activation of CaM. This notion is supported by the fact that these cells do not mobilize Ca^{2+} in response to 5-HT or 8-OH-DPAT in concentrations as high as 5 μM (not shown).

There is a small body of work suggesting that tyrosine phosphorylation of CaM can result in its activation (Sacks et al., 1992; Sacks et al., 1995; De Frutos et al., 1997; Corti et al., 1999). Indeed, we have proposed that G_q-coupled receptors and hypertonicity activate CaM (at

JPET Fast Forward. Published on October 18, 2006 as DOI: 10.1124/jpet.106.112581
This article has not been copyedited and formatted. The final version may differ from this version.

least in part), through its tyrosine phosphorylation (Mukhin et al., 2001; Garnovskaya et al., 2003a; Garnovskaya et al., 2003b). Figure 1C shows that the broad-spectrum tyrosine kinase inhibitor, genistein (100 μM), strongly attenuates the activation of NHE-1 by 100 nM 8-OH-DPAT. In contrast, an inactive congener of genistein (100 μM daidzein) had no effect. These results support the idea that a tyrosine kinase is specifically involved in the activation of NHE-1 by the 5-HT_{1A} receptor. Figure 1D shows that the epidermal growth factor receptor kinase inhibitor, AG1478 (10 μM) had no effect on 5-HT_{1A} receptor-activated NHE-1. In contrast, the Jak2 tyrosine kinase inhibitor, AG490 (40 μM) markedly suppressed NHE-1 activity induced by 100 nM 8-OH-DPAT. These results suggest that both CaM and Jak2 are involved in the activation of NHE-1 by the 5-HT_{1A} receptor.

Roles of Jak2 in the activation of NHE-1 by the 5-HT_{1A} receptor

Figure 2A shows that 100 nM 8-OH-DPAT induces an increase in phosphorylation of Stat3 (an important Jak2 substrate), and that this phosphorylation can be markedly attenuated by the selective 5-HT_{1A} receptor antagonist, S-UH-301 (1 μM). A similar degree of phosphorylation was induced by 100 nM 5-HT, the endogenous ligand of the 5-HT_{1A} receptor (not shown). Additionally, neither 5-HT nor 8-OH-DPAT induced Stat3 phosphorylation in parental CHO-K1 cells not transfected with the 5-HT_{1A} receptor (not shown). Thus, the transfected 5-HT_{1A} receptor mediates Stat3 phosphorylation. Because nearly all signals emanating from the 5-HT_{1A} receptor 8-OH-DPAT are mediated by *Pertussis* toxin (PTX)-sensitive heterotrimeric G proteins ($G_{i/o}\alpha$), we tested the effects of overnight incubation with PTX (200 ng/ml) on the ability of 100 nM to increase Stat3 phosphorylation. Figure 2B shows that PTX completely eliminated 8-OH-DPAT-induced phosphorylation of Stat3. In aggregate, these results demonstrate that the 5-HT_{1A} receptor, acting through $G_{i/o}\alpha$ proteins, induces phosphorylation of Stat3, and thus activation of Jak2, in CHO-K1 cells.

Figure 2C shows that 8-OH-DPAT induces a concentration-dependent increase in the phosphorylation of Stat3, with half maximal stimulation being achieved at ≈30 nM 8-OH-DPAT.

JPET Fast Forward. Published on October 18, 2006 as DOI: 10.1124/jpet.106.112581
This article has not been copyedited and formatted. The final version may differ from this version.

Figure 2D shows that the Jak2 inhibitor, AG490 (40 μM), suppressed 8-OH-DPAT-induced Stat3 phosphorylation by more than 80%. Results obtained by the use of a single pharmacological inhibitor of a target enzyme should be confirmed using other compounds or methods. Thus, we compared the effects of AG490 with those of a highly selective Jak3 inhibitor (JAK3 Inhibitor I, WHI-P131) (Goodman et al., 1998), on the ability of 100 nM to induce phosphorylation of Stat3. Figure 2E shows that AG490 suppressed Stat3 phosphorylation in a concentration-dependent manner by ≈60% at 25 μM and >100% at 100 μM. In contrast, WHI-P131 had no statistically significant effects at concentrations as high as 300 μM. These data demonstrate that the 5-HT_{1A} receptor activates Jak2, and support the possibility that Jak2 plays a key role in the activation of NHE-1 by the 5-HT_{1A} receptor.

One key pathway of activation of NHE-1 is by the formation of protein complexes containing CaM, which binds directly to the carboxyl terminus of NHE-1 and induces a conformational change that unmasks a proton-sensing region of NHE-1 (Wakabayashi et al., 1994a). We used co-immunoprecipitation to provide further evidence supporting a key role for Jak2 in the activation of NHE-1 by the 5-HT_{1A} receptor. Figure 3A shows that the amount of CaM in phosphotyrosine immunoprecipitates was increased by 8-OH-DPAT, and that the increase was attenuated by ≈70% by 40 μM AG490. Similar results were obtained for the converse study (N = 2, not shown), in that the phosphotyrosine content of CaM was increased in response to 100 nM 8-OH-DPAT, and that the increase in phosphotyrosine immunoreactivity was markedly attenuated by 40 μM AG490. Figure 3B shows that there was virtually no association of Jak2 and CaM in Jak2 immunoprecipitates derived from quiescent cells. When cells were stimulated with 100 nM 8-OH-DPAT, there was a large increase in CaM in the Jak2 immunoprecipitates. Moreover, AG490 nearly completely blocked this association. Figure 3C shows similar results when the CaM immunoprecipitates were probed with anti-Jak2 antibodies. We have shown previously that the 5-HT_{1A} receptor binds constitutively to CaM. In order to assess whether Jak2 modulates that binding, we immunoprecipitated the 5-HT_{1A} receptor using an antibody that we have previously characterized (Raymond et al., 1989; Raymond et al.,

1993), following which we probed for the presence of CaM. Figure 3D shows that CaM was associated with the 5-HT_{1A} receptor under basal conditions, and that this association was not significantly altered by treatment with 8-OH-DPAT or with AG490. These results suggest that Jak2 interacts with CaM downstream of the 5-HT_{1A} receptor. Indeed, Figure 3E shows that 8-OH-DPAT increases the amount of CaM in NHE-1 immunoprecipitates, an effect that was attenuated by ≈75% by AG490. This result suggests that Jak2 modulates the interaction of CaM with NHE-1. The results in Figure 3F suggest that Jak2 is present in NHE-1 immunoprecipitates in cells treated with 8-OH-DPAT, and that AG490 attenuates this interaction by ≈70%.

The 5-HT_{1A} receptor activates NHE-1 by inducing a direct interaction of CaM with the NHE-1 carboxyl terminus

Although it is generally accepted that CaM activates NHE-1 by binding directly to its carboxyl terminus (Wakabayashi et al., 1994a), this idea has never been directly tested in living cells. Therefore, we tested this idea using bioluminescence resonance energy transfer (BRET) between CaM and the carboxyl terminus of NHE-1. cDNAs encoding fusion protein constructs were expressed in CHO cells and probed by immunoblot with various antibodies to confirm expression. Figure 4 shows the results of expression of various constructs in CHO cells. Figure 4A shows experiments in which anti-GFP antibodies were used to identify CaM eYFP fusion proteins by immunoblot. Lanes 1 and 10 show immunoblots from lysates derived from mock-transfected CHO cells, and lane 11 shows nontransfected CHO cells. Lanes 2 and 3 show expression of control (non-fused) eYFP-N1 and eYFP-C1 constructs. Lanes 4, 5, 8 and 9 show luciferase fusions, which have no specific immunoreactivity with the GFP antibody. Lanes 6 and 7 show eYFP-N1-CaM and eYFP-C1-CaM, the sizes of which increase by ≈18 kDa, as would be expected for CaM fusions. Figure 4B shows results of immunoblots from the same lysates using an anti-luciferase antibody. Lanes 4 and 5 show control RLuc-N1 and RLuc-C1 constructs. Lanes 8 and 9 show RLuc-N1-CaM and RLuc-C1-CaM, the sizes of which increase by ≈18 kDa, as would be expected for CaM.

JPET Fast Forward. Published on October 18, 2006 as DOI: 10.1124/jpet.106.112581
This article has not been copyedited and formatted. The final version may differ from this version.

We also examined eYFP-CaM and eYFP-NHE-1 constructs by confocal microscopy after expression in CHO cells. Figure 4C shows that eYFP-N1-CaM fusion is dispersed throughout the cell (including the nucleus), with some association with cytoskeletal structures, as would be predicted. The distribution is similar to that of endogenous CaM as revealed with an anti-CaM antibody. In contrast, the eYFP-N1-NHE-1 fusion is distributed primarily on the plasma membrane, and to a lesser extent throughout the cell, but is mainly excluded from the nucleus (Figure 4D). Thus, the most likely location for interaction of NHE-1 and CaM would be on the plasma membrane.

We then used transient co-transfection of BRET pairs in CHO cells expressing the 5-HT_{1A} receptor Results were expressed as the normalized ratio of fluorescence to luminescence in the various wells. Figure 5A shows a positive control experiment in which RLuc alone resulted in little or no BRET signal. Co-transfection of RLuc and eYFP did not generate a BRET signal, indicating that the two molecules do not aggregate with each other to such an extent that they would yield a false positive BRET signal. In contrast, when eYFP was fused either to the amino or carboxyl terminal end of RLuc, measurable signals resulted, with the carboxyl terminal fusion yielding a signal slightly greater than double that generated by the amino terminal fusion.

Figure 5B shows that RLuc fused to NHE-1 (RLuc-N1-NHE-1) yielded virtually no signal. Importantly, when that construct was co-transfected along with eYFP, a small signal (<10 mBU) resulted. This signal is likely the result of non-specific interactions. This signal is relatively small, and is less than 20% of that generated when RLuc-N1-NHE-1 was co-transfected with eYFP-N1-CaM. This suggests that CaM and NHE-1 can interact with each other (come within 100 Å of each other) to a much greater degree than background interactions between RLuc-NHE-1 and non-fused eYFP. To further support the specificity of the interaction between RLuc-N1-NHE-1 and eYFP-N1-CaM, we stimulated CHO-5-HT_{1A}R cells with the selective receptor agonist, 8-OH-DPAT. Treatment with 1 μM 8-OH-DPAT had no effect on the BRET signal in cells expressing RLuc-N1-NHE-1 plus non-fused eYFP, but 8-OH-DPAT treatment induced a 2.5-fold increase in the BRET signal in cells expressing RLuc-N1-NHE-1 plus eYFP-N1-CaM. Similar

results were obtained when cells were transfected with RLuc-N1-CaM plus eYFP-N1-NHE-1, or with RLuc-C1-CaM plus eYFP-N1-NHE-1 (Figure 5C), although the former BRET pair yielded a basal signal double that of the latter pair. In addition, 100 nM 8-OH-DPAT significantly increased the BRET signals for RLuc-N1-CaM plus eYFP-N1-NHE-1, or with RLuc-C1-CaM plus eYFP-N1-NHE-1. The increased BRET signal was significantly attenuated by 40 μM AG490 for both pairs of constructs (Figure 5C), suggesting that Jak2 is involved in the pathway that induces CaM and NHE-1 to associate in live cells. AG490 did not significantly diminish the basal BRET signals (not shown), suggesting that Jak2 is not involved in the constitutive association of CaM and NHE-1. Moreover, a Jak3 inhibitor (200 μM WHI-P131) had no effect (not shown). These studies show that an agonist known to increase NHE-1 activity induces CaM and NHE-1 to come into proximity to each other without inducing non-fused eYFP to come into proximity with NHE-1. Moreover, the strength of the BRET signal depends upon whether luciferase has been fused to the carboxyl or amino terminal end of CaM, as would be expected if the interaction of CaM with NHE-1 were selective, rather than non-specific. The studies also strongly support the involvement of Jak2 in 5-HT_{1A} receptor-induced association of CaM and NHE-1.

JPET Fast Forward. Published on October 18, 2006 as DOI: 10.1124/jpet.106.112581
This article has not been copyedited and formatted. The final version may differ from this version.

Discussion

What is new about this work is that we have shown that a prototypical $G_{i/o}$-coupled receptor, the 5-HT_{1A} receptor, rapidly stimulates NHE-1 through a pathway that involves (1) activation of Jak2 downstream of the 5-HT_{1A} receptor; (2) formation of a complex that includes NHE-1, Jak2, and CaM; (3) tyrosine phosphorylation of CaM through Jak2, and (4) increased binding of CaM to the carboxyl terminus of NHE-1. The evidence for the involvement of CaM is that: (1) five structurally distinct CaM inhibitors markedly attenuate activation of NHE-1 by the 5-HT_{1A} receptor, (2) CaM co-immunoprecipitates with NHE-1, and this is increased by activation of the 5-HT_{1A} receptor by 8-OH-DPAT, and (3) CaM associates with NHE-1 in lives cells as assessed by BRET, and this association increases after stimulation with 8-OH-DPAT. The evidence for the involvement of Jak2 is that: (1) Jak2 is activated rapidly and in a concentration-dependent manner by 8-OH-DPAT, (2) the Jak2 inhibitor, AG490, inhibits 8-OH-DPAT-mediated activation of Stat3 in a concentration-dependent manner, whereas the Jak3 inhibitor, WHI-P131, does not, (3) AG490 inhibits activation of NHE-1 by 8-OH-DPAT, (4) AG490 attenuates tyrosine phosphorylation of CaM induced by 8-OH-DPAT, and (5) AG490 inhibits the association of Jak2 with CaM, CaM with NHE-1, and Jak2 with NHE-1 as assessed by co-immunoprecipitation and/or BRET.

The work is remarkable with regard to several issues. First, the 5-HT_{1A} receptor now joins a handful of G_q-coupled receptors and hypertonic shock as upstream activators of this emerging pathway. Second, we have presented clear evidence that CaM can be activated through tyrosine phosphorylation in the absence of a significant role for elevated intracellular Ca^{2+}. Third, we have demonstrated for the first time that the association of CaM with NHE-1 in living cells is a dynamic process.

We have previously demonstrated that the bradykinin B_2, 5-HT_{2A}, and angiotensin II AT_{1A} receptors, all of which couple to $G_{q/11}\alpha$, can rapidly activate NHE-1 through a novel pathway that involves coordinated activities of CaM and Jak2 (Garnovskaya et al., 1998; Garnovskaya et al.,

2003a). Additionally, we have shown that exposure of cells to hypertonic media activates NHE-1 through a similar mechanism (Garnovskaya et al., 2003b). One key difference is that the $G_{q/11}\alpha$-coupled receptors engage this pathway to some extent through elevated intracellular Ca^{2+}, whereas hypertonic medium engages this pathway independent of elevated intracellular Ca^{2+}. The current study demonstrates that the $G_{i/o}\alpha$-coupled 5-HT_{1A} receptor also activates NHE-1 through CaM and Jak2. However, the pathway more closely resembles that induced by hypertonic exposure in that elevations of intracellular Ca^{2+} are not involved. Thus, the results demonstrate that CaM and Jak2 link $G_{i/o}\alpha$-coupled receptors, as well as $G_{q/11}\alpha$-coupled receptors and hypertonic medium, to NHE-1 activation. They also demonstrate that significant elevations of intracellular Ca^{2+} are not necessary for CaM to play a critical role in the activation of NHE-1.

CaM has been previously shown to be a substrate for phosphorylation by both tyrosine kinases and serine-threonine kinases (Sacks et al., 1992; Sacks et al., 1995; Corti et al., 1999). Activation of the insulin receptor (a receptor tyrosine kinase) has been shown to result in phosphorylation of Tyr-99 and Tyr-138 of CaM in CHO-IR cells (De Frutos et al., 1997). The epidermal growth factor receptor (another receptor tyrosine kinase) phosphorylates Tyr-99 of bovine brain CaM (De Frutos et al., 1997; Benaim and Villalobo, 2002) with a stoichiometry of 1:1. In contrast, casein kinase II, an insulin-sensitive non-receptor kinase, phosphorylates CaM *in vitro* on serine and threonine residues (Thr-79, Ser-81, Ser-101 and Thr-117) (Sacks et al., 1992). We recently demonstrated that CaM could serve as a substrate for purified Jak2 (Mukhin et al., 2001), although the current work does not definitively demonstrate a direct role for Jak2 in the tyrosine phosphorylation of CaM after activation of the 5-HT_{1A} receptor. It is noteworthy that both insulin and epidermal growth factor receptors have been shown to phosphorylate CaM on Tyr-99 and/or Tyr-138 of CaM (De Frutos et al., 1997; Benaim and Villalobo, 2002); these are the only tyrosine residues within CaM. Based on the crystal structure of CaM, Tyr-99 is located within the third Ca^{2+}-binding domain, and is somewhat more exposed than is Tyr-138 (Benaim and Villalobo, 2002).

JPET Fast Forward. Published on October 18, 2006 as DOI: 10.1124/jpet.106.112581
This article has not been copyedited and formatted. The final version may differ from this version.

There is no consensus on the effects of phosphorylation of CaM on its ability to interact with and activate its downstream targets. Our work suggests that tyrosine phosphorylation of CaM results in increased binding to and activation of NHE-1. Unlike our studies, Fukami *et al.* previously suggested that Ca^{2+}-induced phosphorylation of CaM may attenuate its function *in vivo* (Fukami et al., 1986). Phosphorylation of CaM on Tyr-99 was shown to selectively attenuate the action of CaM antagonists on type-I cyclic nucleotide phosphodiesterase activity (Saville and Houslay, 1994). In contrast, phosphorylation of Tyr-99 increases the affinity of CaM for Ca^{2+}-ATPase (Sacks et al., 1996). In order to address that discrepancy, Corti *et al.* studied the effects of CaM phosphorylated on Tyr-99 on the binding affinities and activation of six different CaM target enzymes (myosin light chain kinase, 3'-5'-cyclic nucleotide phosphodiesterase, plasma membrane Ca^{2+}-ATPase, Ca^{2+}-CaM dependent protein phosphatase 2B [calcineurin], neuronal nitric oxide synthase and type II Ca^{2+}-CaM dependent protein kinase) (Corti et al., 1999). They concluded that tyrosine phosphorylation of CaM Tyr-99 generally led to an increase in the ability of CaM to activate its targets. For three of the enzymes (3'-5'-cyclic nucleotide phosphodiesterase, plasma membrane Ca^{2+}-ATPase, and type II Ca^{2+}-CaM dependent protein kinase) the primary effect was a decrease in the concentration at which half-maximal activation was attained. In contrast, for calcineurin and neuronal nitric oxide synthase, phosphorylation of CaM significantly increased the V_{max}. For myosin light chain kinase, however, tyrosine phosphorylation of CaM had no effect (Corti et al., 1999). Thus, the idea that tyrosine phosphorylation of CaM results in increased binding to and activation of NHE-1 is supported by precedent with other CaM-activated enzymes.

The idea that the activation of NHE-1 by CaM involves a conformational change in NHE-1 that unmasks its proton-sensing and/or transport region was supported by early mutagenesis work by Pouyssegur's group (Wakabayashi et al., 1994a; Wakabayashi et al., 1994b; Wakabayashi et al., 1995; Wakabayashi et al., 2003). However, the direct observation of the dynamic interaction between NHE-1 and CaM in living cells has heretofore not been demonstrated. Our work fills that gap in the knowledge base in that 5-HT_{1A} receptor activation

leads to an increased BRET signal between CaM and the carboxyl terminus of NHE-1. Clearly, considerable structural work remains to be done to fully test the ideas proposed by Pouyssegur's group. However, when taken together with our previous work (Garnovskaya et al., 1997) and that of Pouyssegur's group, the following pathway of activation of NHE-1 is likely: 5-HT_{1A} receptor → $G_{i2}\alpha$ and/or $G_{i3}\alpha$ → Jak2 activation → tyrosine phosphorylation of CaM → increased binding of CaM to NHE-1 → induction of a conformational change in NHE-1 that unmasks an obscured proton-sensing and/or proton transporting region of NHE-1 → activation of NHE-1.

Acknowledgments

The authors gratefully acknowledge assistance and advice from Georgiann Collinsworth.

References

Benaim G and Villalobo A (2002) Calmodulin phosphorylation. *Eur J Biochem* **269**:3619-3631.

Corti C, Leclerc L'Hostis E, Quadroni M, Schmid H, Durussel I, Cox J, Dainese Hatt P, James P and Carafoli E (1999) Tyrosine phosphorylation modulates the interaction of calmodulin with its target proteins. *Eur J Biochem* **262**:790-802.

Counillon L and Pouyssegur J (2000) The expanding family of eucaryotic Na^+/H^+ exchangers. *J Biol Chem* **275**:1-4.

Crivici A and Ikura M (1995) Molecular and structural basis of target recognition by calmodulin. *Annu Rev Biophys Biomol Struct* **24**:85-116.

De Frutos T, Martin-Nieto J and Villalobo A (1997) Phosphorylation of calmodulin by permeabilized fibroblasts overexpressing the human epidermal growth factor receptor. *Biol Chem* **378**:31-37.

Fliegel L (2005) The Na^+/H^+ exchanger isoform 1. *Int J Biochem Cell Biol* **37**:33-37.

Fliegel L, Walsh MP, Singh D, Wong C and Barr A (1992) Phosphorylation of the C-terminal domain of the Na^+/H^+ exchanger by Ca^{2+}/calmodulin-dependent protein kinase II. *Biochem J* **282 (Pt 1)**:139-145.

Fukami Y, Nakamura T, Nakayama A and Kanehisa T (1986) Phosphorylation of tyrosine residues of calmodulin in Rous sarcoma virus-transformed cells. *Proc Natl Acad Sci U S A* **83**:4190-4193.

Garciandia A, Lopez R, Tisaire J, Arrazola A, Fortuno A, Bueno J and Diez J (1995) Enhanced Na^+-H^+ exchanger activity and NHE-1 mRNA expression in lymphocytes from patients with essential hypertension. *Hypertension* **25**:356-364.

Garnovskaya MN, Gettys TW, van Biesen T, Prpic V, Chuprun JK and Raymond JR (1997) 5-HT_{1A} receptor activates Na^+/H^+ exchange in CHO-K1 cells through $G_{i\alpha 2}$ and $G_{i\alpha 3}$. *J Biol Chem* **272**:7770-7776.

Garnovskaya MN, Mukhin Y and Raymond JR (1998) Rapid activation of sodium-proton exchange and extracellular signal-regulated protein kinase in fibroblasts by G protein-coupled 5-HT_{1A} receptor involves distinct signalling cascades. *Biochem J* **330 (Pt 1)**:489-495.

Garnovskaya MN, Mukhin YV, Turner JH, Vlasova TM, Ullian ME and Raymond JR (2003a) Mitogen-induced activation of Na^+/H^+ exchange in vascular smooth muscle cells involves janus kinase 2 and Ca^{2+}/calmodulin. *Biochemistry* **42**:7178-7187.

Garnovskaya MN, Mukhin YV, Vlasova TM and Raymond JR (2003b) Hypertonicity activates Na^+/H^+ exchange through Janus kinase 2 and calmodulin. *J Biol Chem* **278**:16908-16915.

Goodman PA, Niehoff LB and Uckun FM (1998) Role of tyrosine kinases in induction of the c-jun proto-oncogene in irradiated B-lineage lymphoid cells. *J Biol Chem* **273**:17742-17748.

Grinstein S, Rotin D and Mason MJ (1989) Na^+/H^+ exchange and growth factor-induced cytosolic pH changes. Role in cellular proliferation. *Biochim Biophys Acta* **988**:73-97.

Karmazyn M, Liu Q, Gan XT, Brix BJ and Fliegel L (2003) Aldosterone increases NHE-1 expression and induces NHE-1-dependent hypertrophy in neonatal rat ventricular myocytes. *Hypertension* **42**:1171-1176.

McConnell HM, Owicki JC, Parce JW, Miller DL, Baxter GT, Wada HG and Pitchford S (1992) The cytosensor microphysiometer: biological applications of silicon technology. *Science* **257**:1906-1912.

Mukhin YV, Vlasova T, Jaffa AA, Collinsworth G, Bell JL, Tholanikunnel BG, Pettus T, Fitzgibbon W, Ploth DW, Raymond JR and Garnovskaya MN (2001) Bradykinin B_2

receptors activate Na^+/H^+ exchange in mIMCD-3 cells via Janus kinase 2 and Ca^{2+}/calmodulin. *J Biol Chem* **276**:17339-17346.

Pouyssegur J, Sardet C, Franchi A, L'Allemain G and Paris S (1984) A specific mutation abolishing Na^+/H^+ antiport activity in hamster fibroblasts precludes growth at neutral and acidic pH. *Proc Natl Acad Sci U S A* **81**:4833-4837.

Putney LK, Denker SP and Barber DL (2002) The changing face of the Na^+/H^+ exchanger, NHE1: structure, regulation, and cellular actions. *Annu Rev Pharmacol Toxicol* **42**:527-552.

Raymond JR, Fargin A, Lohse MJ, Regan JW, Senogles SE, Lefkowitz RJ and Caron MG (1989) Identification of the ligand-binding subunit of the human 5-hydroxytryptamine$_{1A}$ receptor with N-(p-azido-m-[^{125}I] iodophenethyl)spiperone, a high affinity radioiodinated photoaffinity probe. *Mol Pharmacol* **36**:15-21.

Raymond JR, Kim J, Beach RE and Tisher CC (1993) Immunohistochemical mapping of cellular and subcellular distribution of 5-HT$_{1A}$ receptors in rat and human kidneys. *Am J Physiol* **264**:F9-19.

Sacks DB, Davis HW, Crimmins DL and McDonald JM (1992) Insulin-stimulated phosphorylation of calmodulin. *Biochem J* **286 (Pt 1)**:211-216.

Sacks DB, Lopez MM, Li Z and Kosk-Kosicka D (1996) Analysis of phosphorylation and mutation of tyrosine residues of calmodulin on its activation of the erythrocyte Ca^{2+}-transporting ATPase. *Eur J Biochem* **239**:98-104.

Sacks DB, Mazus B and Joyal JL (1995) The activity of calmodulin is altered by phosphorylation: modulation of calmodulin function by the site of phosphate incorporation. *Biochem J* **312 (Pt 1)**:197-204.

Sardet C, Fafournoux P and Pouyssegur J (1991) Alpha-thrombin, epidermal growth factor, and okadaic acid activate the Na^+/H^+ exchanger, NHE-1, by phosphorylating a set of common sites. *J Biol Chem* **266**:19166-19171.

Sauvage M, Maziere P, Fathallah H and Giraud F (2000) Insulin stimulates NHE1 activity by sequential activation of phosphatidylinositol 3-kinase and protein kinase C zeta in human erythrocytes. *Eur J Biochem* **267**:955-962.

Saville MK and Houslay MD (1994) Phosphorylation of calmodulin on Tyr99 selectively attenuates the action of calmodulin antagonists on type-I cyclic nucleotide phosphodiesterase activity. *Biochem J* **299 (Pt 3)**:863-868.

Shrode LD, Klein JD, O'Neill WC and Putnam RW (1995) Shrinkage-induced activation of Na^+/H^+ exchange in primary rat astrocytes: role of myosin light-chain kinase. *Am J Physiol* **269**:C257-266.

Takahashi E, Abe J, Gallis B, Aebersold R, Spring DJ, Krebs EG and Berk BC (1999) p90(RSK) is a serum-stimulated Na^+/H^+ exchanger isoform-1 kinase. Regulatory phosphorylation of serine 703 of Na^+/H^+ exchanger isoform-1. *J Biol Chem* **274**:20206-20214.

Tominaga T, Ishizaki T, Narumiya S and Barber DL (1998) p160ROCK mediates RhoA activation of Na-H exchange. *Embo J* **17**:4712-4722.

Turner JH, Gelasco AK and Raymond JR (2004) Calmodulin interacts with the third intracellular loop of the serotonin 5-hydroxytryptamine$_{1A}$ receptor at two distinct sites: putative role in receptor phosphorylation by protein kinase C. *J Biol Chem* **279**:17027-17037.

Turner JH and Raymond JR (2005) Interaction of calmodulin with the serotonin 5-hydroxytryptamine$_{2A}$ receptor. A putative regulator of G protein coupling and receptor phosphorylation by protein kinase C. *J Biol Chem* **280**:30741-30750.

Wakabayashi S, Bertrand B, Ikeda T, Pouyssegur J and Shigekawa M (1994a) Mutation of calmodulin-binding site renders the Na^+/H^+ exchanger (NHE1) highly H^+-sensitive and Ca^{2+} regulation-defective. *J Biol Chem* **269**:13710-13715.

Wakabayashi S, Bertrand B, Shigekawa M, Fafournoux P and Pouyssegur J (1994b) Growth factor activation and "H^+-sensing" of the Na^+/H^+ exchanger isoform 1 (NHE1). Evidence

for an additional mechanism not requiring direct phosphorylation. *J Biol Chem* **269**:5583-5588.

Wakabayashi S, Hisamitsu T, Pang T and Shigekawa M (2003) Mutations of Arg440 and Gly455/Gly456 oppositely change pH sensing of Na^+/H^+ exchanger 1. *J Biol Chem* **278**:11828-11835.

Wakabayashi S, Ikeda T, Noel J, Schmitt B, Orlowski J, Pouyssegur J and Shigekawa M (1995) Cytoplasmic domain of the ubiquitous Na^+/H^+ exchanger NHE1 can confer Ca^{2+} responsiveness to the apical isoform NHE3. *J Biol Chem* **270**:26460-26465.

Wang Y, Meyer JW, Ashraf M and Shull GE (2003) Mice with a null mutation in the NHE1 Na^+-H^+ exchanger are resistant to cardiac ischemia-reperfusion injury. *Circ Res* **93**:776-782.

Xu Y, Piston DW and Johnson CH (1999) A bioluminescence resonance energy transfer (BRET) system: application to interacting circadian clock proteins. *Proc Natl Acad Sci U S A* **96**:151-156.

Yan W, Nehrke K, Choi J and Barber DL (2001) The Nck-interacting kinase (NIK) phosphorylates the Na^+-H^+ exchanger NHE1 and regulates NHE1 activation by platelet-derived growth factor. *J Biol Chem* **276**:31349-31356.

Footnotes

This work was supported by grants from the Department of Veterans Affairs (Merit Awards and a REAP award to JRR and MNG), the National Institutes of Health (GM08716 to JHT, DK52448 and GM63909 to JRR), a pre-doctoral fellowship from the American Heart Association, Mid Atlantic Affiliate (0215195U to JHT), and laboratory endowments jointly supported by the M.U.S.C. Division of Nephrology and Dialysis Clinics, Inc. (JRR).

Address correspondence to Dr. John Raymond, 179 Ashley Avenue, Office of the Provost, Charleston, SC, 29425. Phone 1-(843)-792-3031, Fax 1-(843)-792-5110, e-mail raymondj@musc.edu.

JPET Fast Forward. Published on October 18, 2006 as DOI: 10.1124/jpet.106.112581
This article has not been copyedited and formatted. The final version may differ from this version.

Legends for Figures

Figure 1. The 5-HT_{1A} receptor stimulates NHE-1 *via* a CaM- and Jak2-dependent mechanism. CHO-5-HT_{1A}R cells were placed in microphysiometer chambers and were treated with 100 nM 8-OH-DPAT for 6 min after obtaining baseline reading for 6 min. Some chambers were pre-treated with inhibitors for 15 min prior to establishing baseline readings. A, Representative tracings show that incubation with 1 μM ophiobolin A (open circles) attenuates 8-OH-DPAT mediated increases in the extracellular acidification rate (ECAR) (filled circles). B, Summary data expressed as mean ± SEM of four independent experiments testing the effects of each of five CaM inhibitors (5 μM calmidazolium, 1 μM ophiobolin A, 50 μM W-7, 10 μM fluphenazine, and 10 μM chlorpromazine), and the calcium chelating agent, BAPTA-AM (50 μM), on 8-OH-DPAT-induced ECAR. C, Representative tracings show that incubation with 100 μM genistein (a broad spectrum tyrosine kinase inhibitor, open squares), attenuates 8-OH-DPAT mediated increases in ECAR (black filled squares), whereas an inactive congener of genistein (100 μM daidzein, gray filled squares), does not. D, Summary data expressed as mean ± SEM of three independent experiments testing the effects of each of four tyrosine kinase inhibitors (100 μM daidzein or genistein, 40 μM AG490, and 10 μM AG1478), on 8-OH-DPAT-induced ECAR. * indicates $p < 0.05$ after using the Bonferroni correction for multiple comparisons on paired, one-tailed *t*-tests.

Figure 2. The 5-HT_{1A} receptor stimulates Jak2. Phosphorylation of Stat3 (a Jak2 substrate) was assessed by immunoblots with phospho-Stat3-Y705 antibodies. A, Mean ± SEM of four experiments in which CHO-5-HT_{1A}R cells were stimulated for 5 min with 100 nM 8-OH-DPAT in the presence and absence of 1 μM S-UH-301, an antagonist of the 5-HT_{1A} receptor. Top inset shows a representative phospho-Stat3-Y705 immunoblot, whereas the bottom inset shows a representative total Stat3 blot, documenting equal loading. B, Same as in A, except that cells were treated (or not) with 200 ng/ml of *Pertussis* toxin prior to stimulation for 5 min with 100 nM

8-OH-DPAT. Experiments were performed three separate times. C, Concentration-response plot of three experiments studying the effects of 8-OH-DPAT on Stat3 phosphorylation. D, Summary of three experiments performed as described in A, except that cells were pre-incubated (or not) with 40 µM AG490, a Jak2 inhibitor. * indicates $p < 0.05$ *vs* basal after using the Bonferroni correction for multiple comparisons on paired, one-tailed t-tests. E, Summary of three experiments comparing the effects of increasing concentrations of AG490 (gray bars), and WHI-P131 (a Jak3 inhibitor, hatched bars), on Stat3 phosphorylation induced by 100 nM 8-OH-DPAT. ** indicates $p < 0.05$ *vs* 100 nM 8-OH-DPAT after using the Bonferroni correction for multiple comparisons on unpaired, one-tailed *t*-tests. ND = not done.

Figure 3. Immunoprecipitation-immunoblots. Experiments were performed as described in the Methods section. A-F, CHO-5-HT_{1A}R cells were pre-incubated (or not) with 40 µM AG490 prior to stimulation with 100 nM 8-OH-DPAT. Soluble lysates were subjected to immunoprecipitation (IP), following which the immunoprecipitates were subjected to immunoblotting (IB). For each panel, a representative inset is provided, and the summary of three experiments for each is presented as mean ± SEM. * indicates $p < 0.05$ on paired, one-tailed *t*-tests *vs* vehicle-treated cells. ** indicates $p < 0.05$ *vs* 100 nM 8-OH-DPAT on paired, one-tailed *t*-tests. Antibodies used were targeted against PY (phosphotyrosine), CaM (calmodulin), Jak2 (Janus kinase 2), 5-HT_{1A}R (5-HT_{1A} receptor), NHE-1 (sodium-proton exchanger type 1).

Figure 4. Characterization of BRET constructs. A and B, Immunoblots with antibodies against GFP and luciferase, of extracts derived from CHO-K1 cells transfected with the indicated fusion proteins. C, Comparative fluorescence microscopy of CaM-eYFP and endogenous CaM in CHO-K1 cells. D. Fluorescence microscopy of NHE-1-eYFP in CHO-K1 cells.

Figure 5. Interaction of NHE-1 and CaM in live CHO-5-HT_{1A}R cells as assessed by BRET. CHO-5-HT_{1A}R cells were plated at 1×10^5 cells per well in six-well plates, allowed to attach for

24 h, and then were transfected with 2 μg/well of each of the indicated cDNAs using lipofectAMINE 2000 (Invitrogen, Carlsbad, CA). BRET ratios were measured 48 h later as described in the Methods section. A. Negative and positive controls (left two and right two bars, respectively). B. Negative controls (left three bars), evidence for association of CaM and NHE-1 in live cells (second bar from the right), and agonist-induced increase in BRET signal (right-most bar). C. Evidence that 8-OH-DPAT-induced increases in BRET signal between NHE-1 and CaM can be attenuated by a Jak2 inhibitor. Results shown are means ± SEM of at least three independent experiments for each panel. Results are described in detail in the text.

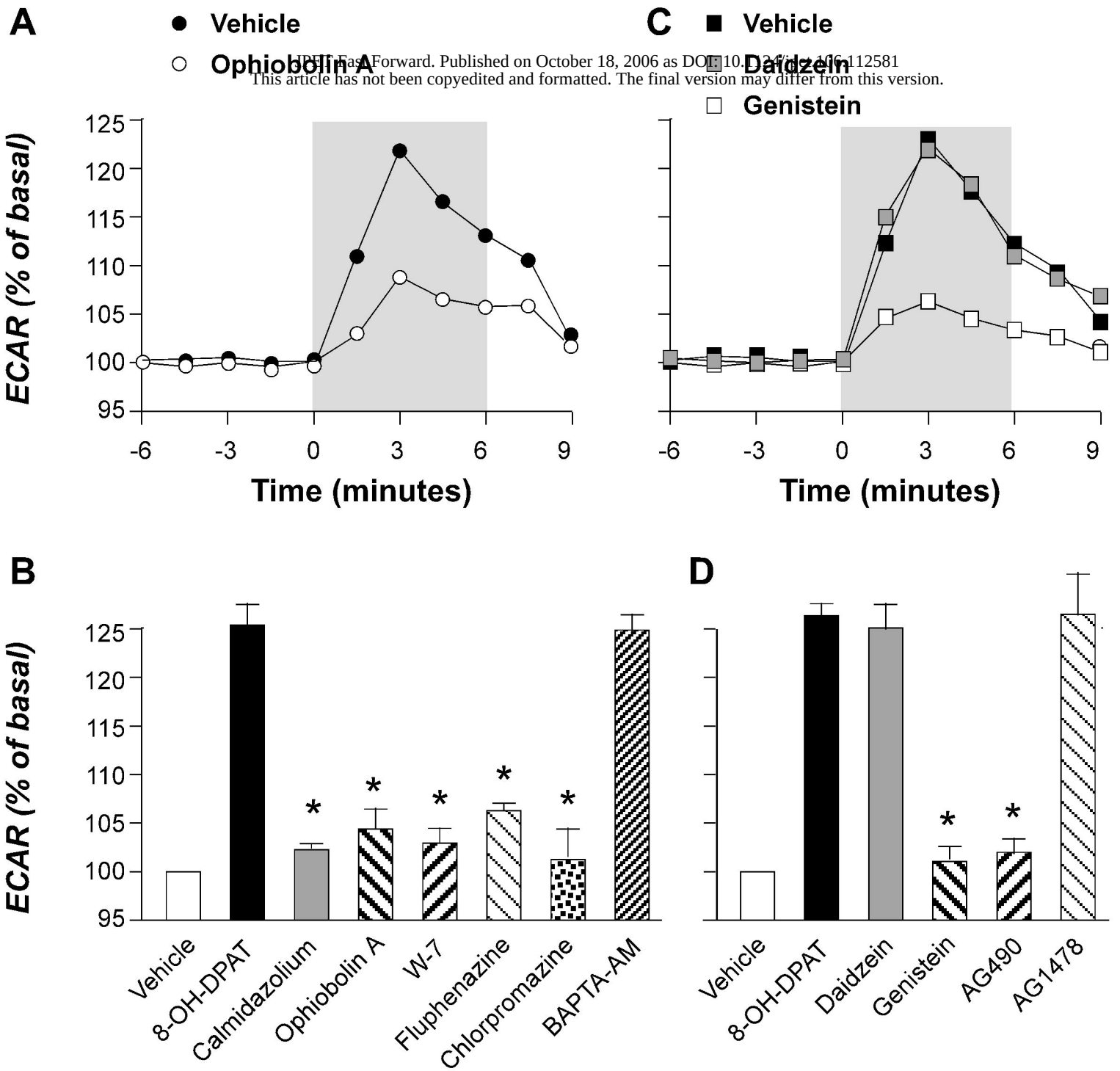

Figure 1

JPET Fast Forward. Published on October 18, 2006 as DOI: 10.1124/jpet.106.112581
This article has not been copyedited and formatted. The final version may differ from this version.

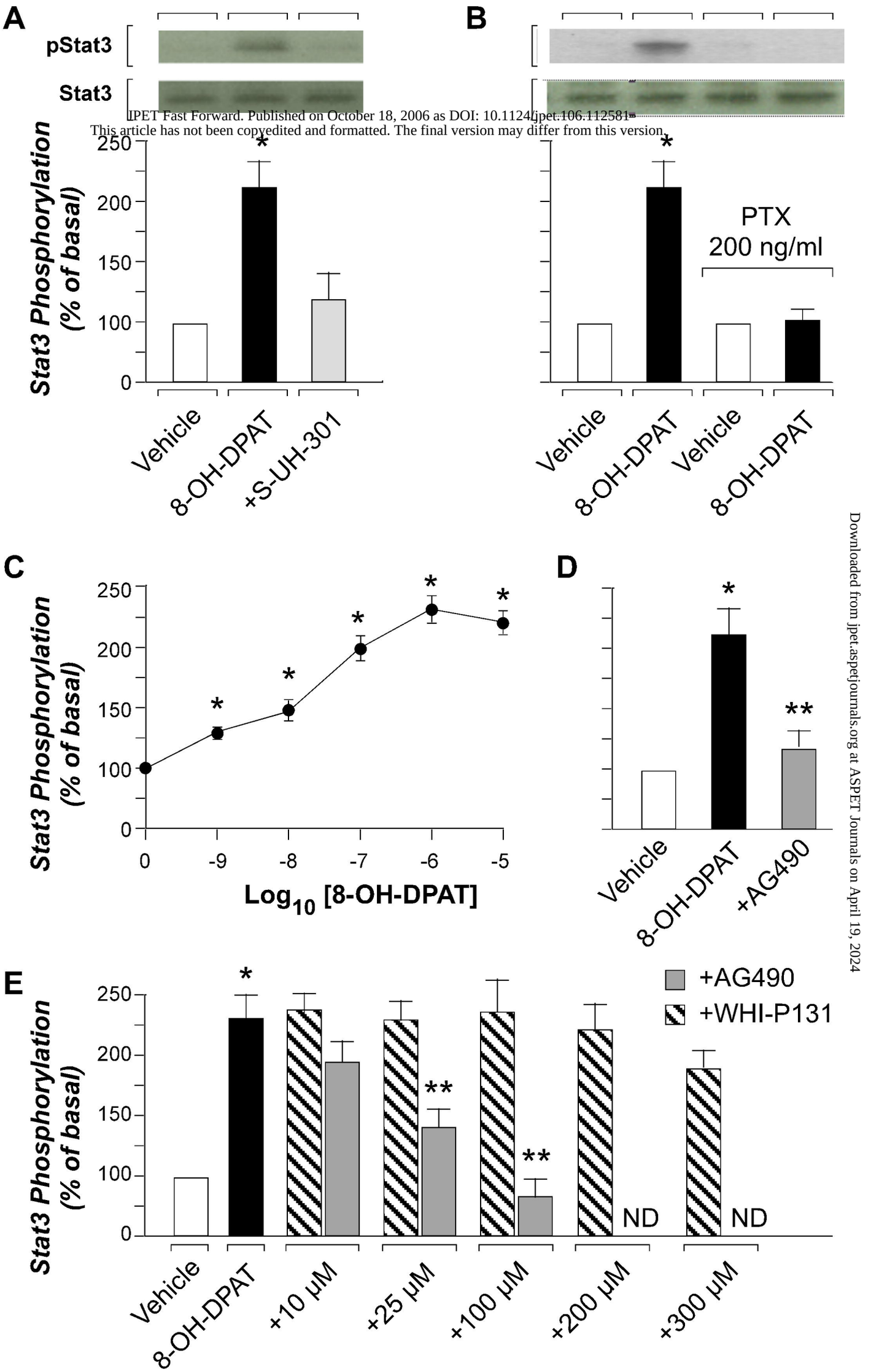

Figure 2

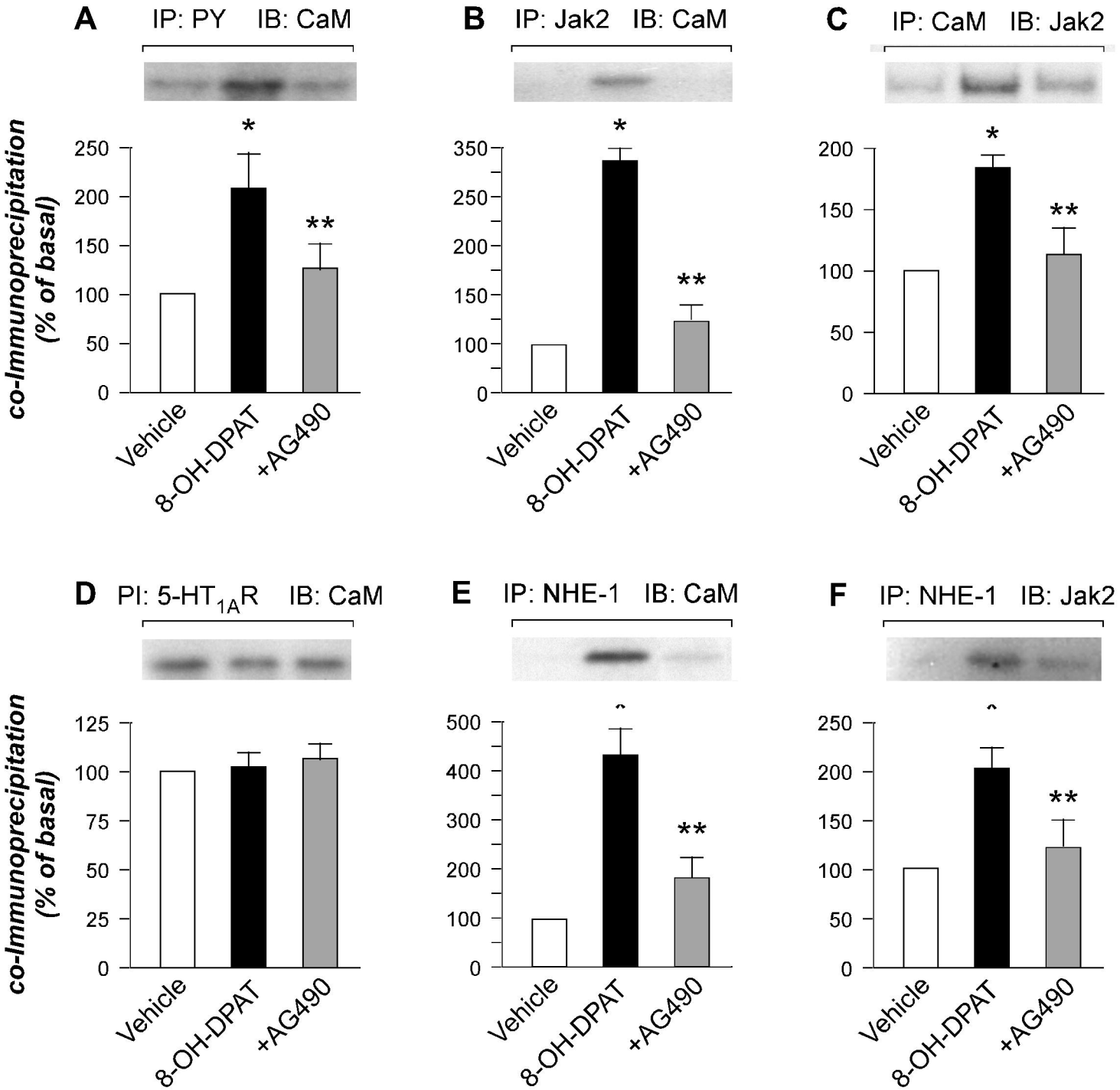
A
IP: PY IB: CaM
B
IP: Jak2 IB: CaM
C
IP: CaM IB: Jak2
co-Immunoprecipitation (% of basal)
250
200
150
100
50
0
350
250
200
150
100
0
*
**
Vehicle
8-OH-DPAT
+AG490
D
PI: 5-HT1AR IB: CaM
E
IP: NHE-1 IB: CaM
F
IP: NHE-1 IB: Jak2
125
100
75
50
25
500
400
300

Figure 3

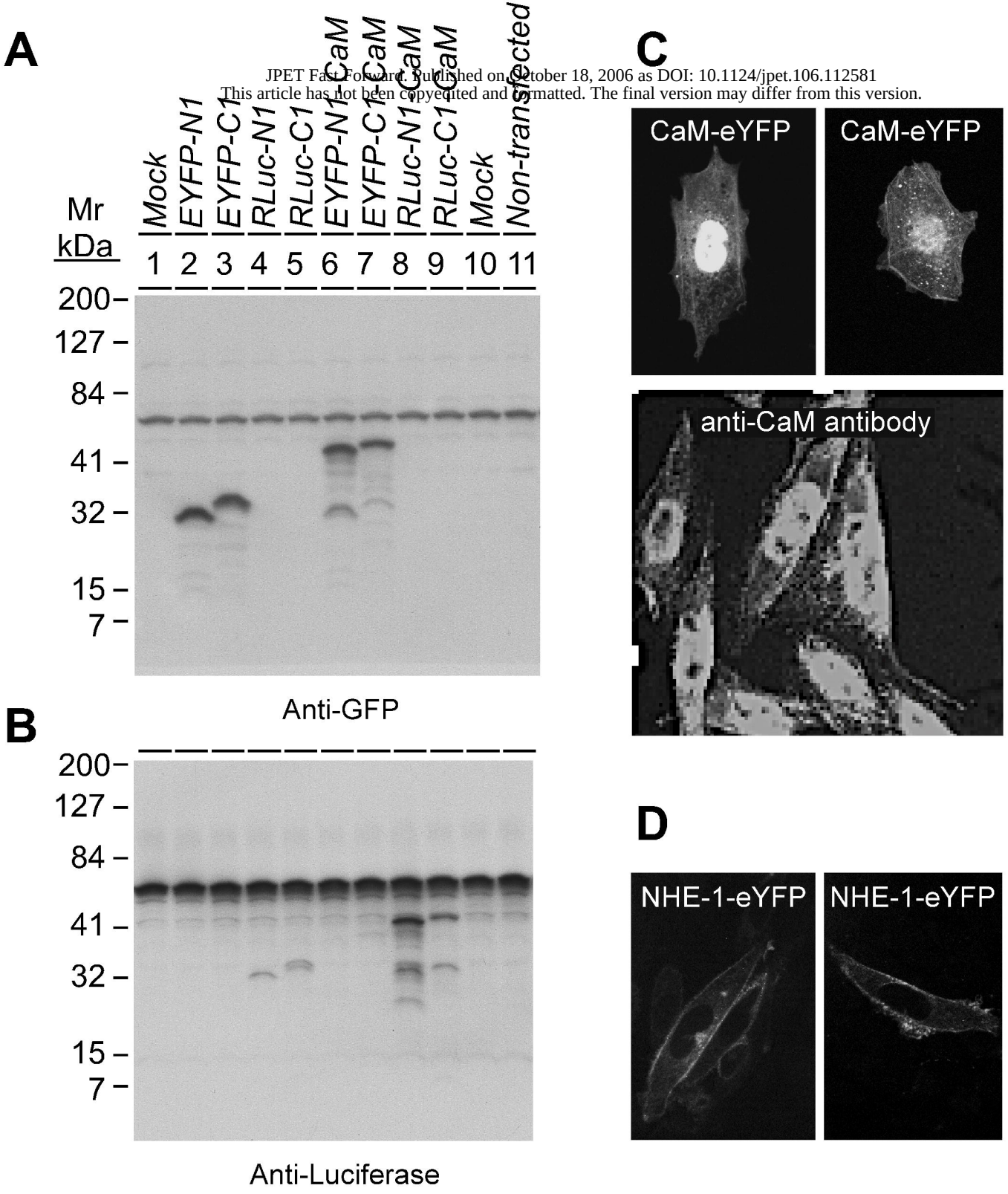

Figure 4

JPET Fast Forward. Published on October 18, 2006 as DOI: 10.1124/jpet.106.112581

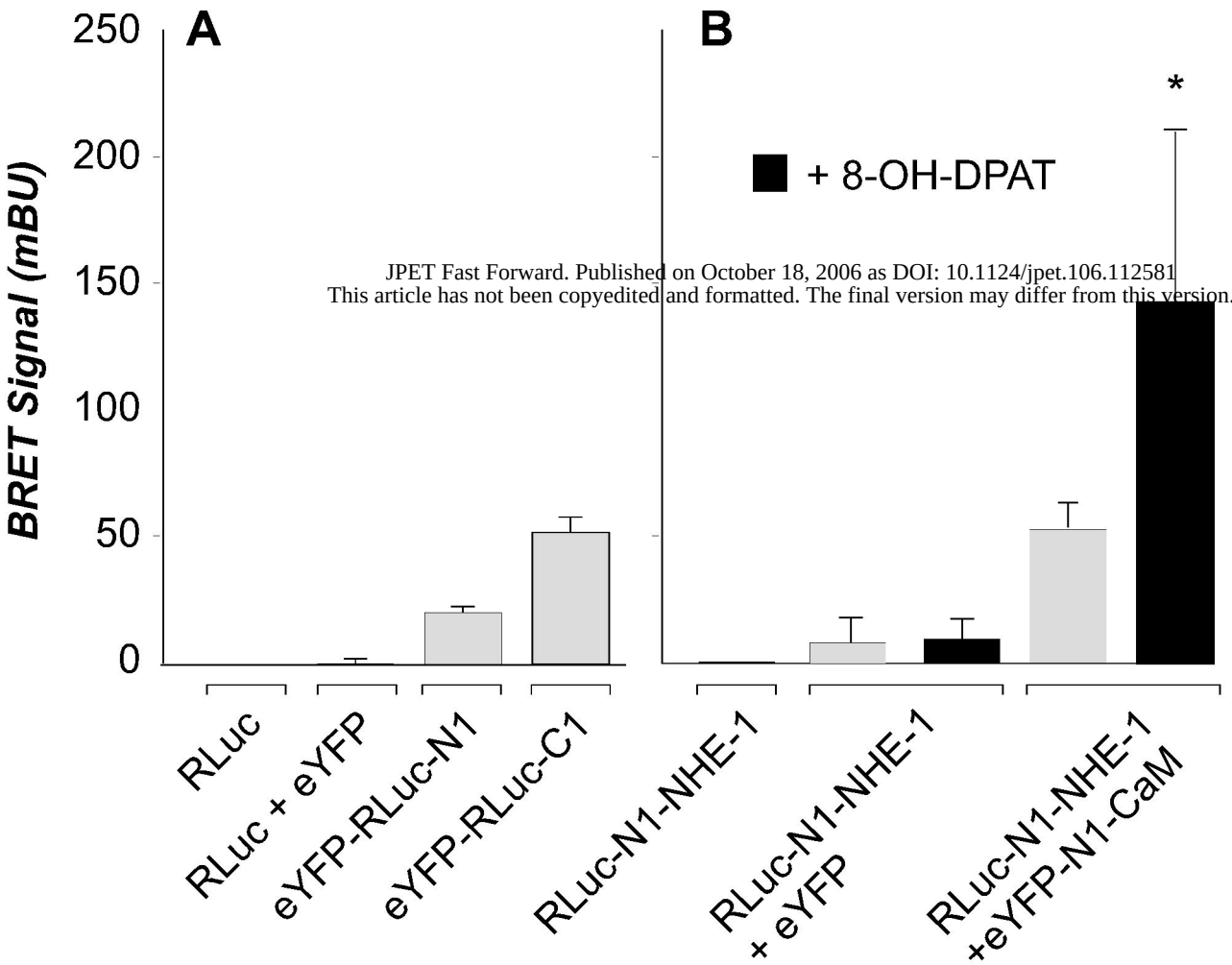

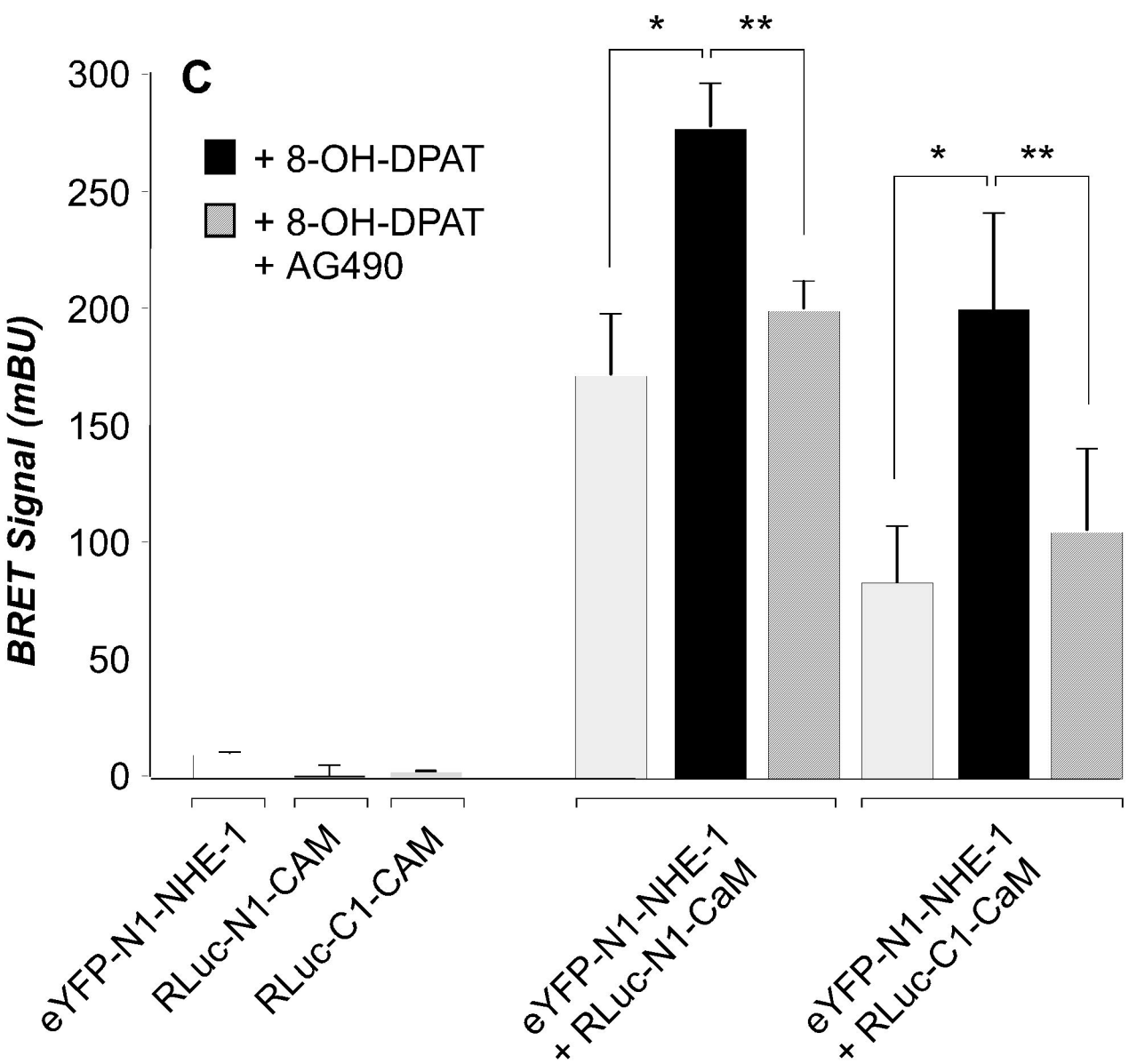

Figure 5